Nuclear Medicine and Biology 44 (2017) 62–68

Contents lists available at ScienceDirect

Nuclear Medicine and Biology

journal homepage: www.elsevier.com/locate/nucmedbio

Radiolabeling and biological characterization of TPGS-based nanomicelles by means of small animal imaging

Fiorella Carla Tesan [a,*], Mariano Gastón Portillo [a], Marcela Analía Moretton [b,c], Ezequiel Bernabeu [b,c], Diego Andrés Chiappetta [b,c], Maria Jimena Salgueiro [a], Marcela Beatriz Zubillaga [a,b]

[a] Physics Department, Facultad de Farmacia y Bioquímica, Universidad de Buenos Aires, Argentina
[b] Consejo Nacional de Investigaciones Científicas y Técnicas (CONICET), Buenos Aires, Argentina
[c] Department of Pharmaceutical Technology, Facultad de Farmacia y Bioquímica, Universidad de Buenos Aires

ARTICLE INFO

Article history:
Received 8 February 2016
Received in revised form 29 September 2016
Accepted 29 September 2016

Keywords:
TPGS
Nanomicelles
^{99m}Tc
Small animal imaging
Biodistribution

ABSTRACT

Introduction: In recent years, nanomedicines have raised as a powerful tool to improve prevention, diagnosis and treatment of different pathologies. Among the most well investigated biomaterials, D-α-tocopheryl polyethylene glycol succinate (also known as TPGS) has been on the spot for the last decade. We therefore designed a method to biologically characterize TPGS-based nanomicelles by labeling them with ^{99m}Tc.
Methods: Labeling process was performed by a direct method. The average hydrodynamic diameter of TPGS nanomicelles was measured by dynamic light scattering and radiochemical purity was assessed by thin layer chromatography. Imaging: a dynamic study was performed during the first hour post radioactive micelles administration in a gamma camera (TcO_4^- was also administered for comparative purposes). Then two static images were acquired in ventral position: 1 h and 12 h post injection. Blood pharmacokinetics of ^{99m}Tc-TPGS during 24 h was performed.
Results: Images revealed whole body biodistribution at an early and delayed time and semiquantification was performed in organs of interest (%Total counts: soft tissue 6.1 ± 0.5; 3.9 ± 0.1, Bone 1.2 ± 0.2; 1 ± 0.1, Heart 1.5 ± 0.6; 0.7 ± 0.3, Kidneys 16.6 ± 1.3; 26.5 ± 1.7, Liver 8.6 ± 1.1; 11.1 ± 0.1 for 1 and 12 h post injection respectively).
Conclusion: This work demonstrated that TPGS based nanomicelles are susceptible to be radiolabeled with ^{99m}Tc thus they can be used to perform imaging studies in animal models. Moreover radiolabeling of these delivery nano systems reveals their possibility to be used as diagnostic agents in the near future.

1. Introduction

In recent years, nanomedicines have raised as a powerful tool to improve prevention, diagnosis and treatment of different pathologies. Their nano-sized range along with their high surface-to-volume ratio and their favorable physico-chemical characteristics makes them suitable for modulation of the pharmacokinetic and pharmacodynamic drug profiles. In this context nanotechnology offers a variety of strategies to develop novel drug delivery systems with not only an improved drug aqueous solubility and chemical stability, but also with controlled drug release and preferential accumulation in certain tissues or in solid tumors (passive or active targeting) [1,2].

Among the most well investigated biomaterials, D-α-tocopheryl polyethylene glycol succinate (also known as TPGS) has been on the spot for the last decade. It is the water-soluble form of vitamin E, resulting from the esterification of vitamin E succinate with polyethylene glycol 1000. It exhibits an average molecular weight of 1513 Da and a hydrophile–lipophile balance value of 13.2 (amphiphilic nature). TPGS is a generally regarded as safe (GRAS)-listed oral supplement which has been approved by the FDA as a safe pharmaceutical adjuvant used in drug formulation [3].

Due to TPGS properties as an absorption/permeation enhancer, emulsifier, solubilizer and stabilizer agent, it has been investigated for the development of a wide variety of drug delivery systems including micelles, TPGS-based nanoparticles (NPs), liposomes, nanosuspensions, solid dispersions and TPGS-based pro-drugs. For instance, TPGS-based block copolymers NPs have been studied to antineoplastic drugs delivery [4]. Also TPGS surface-decorated NPs have been employed for paclitaxel delivery [5]. Due to TPGS amphiphilic nature, it has been explored as a micelle-forming biomaterial, especially for oral and parenteral administration in antineoplastic therapy [6–10]. In this context, it has been reported that TPGS could serve as a pharmaceutical additive for overcoming multidrug resistance and as an inhibitor of P-glycoprotein for increasing the cytotoxicity and bioavailability of anticancer drugs [5,11,12]. It has also been investigated for the treatment of other pathologies including the drug delivery of antiretrovirals and calcium channel blockers [13,14].

* Corresponding author at: Junín 956, PC 1113, Argentina. Tel.: +54 11 49648202.
E-mail address: ftesan@ffyb.uba.ar (F.C. Tesan).

http://dx.doi.org/10.1016/j.nucmedbio.2016.09.006
0969-8051/

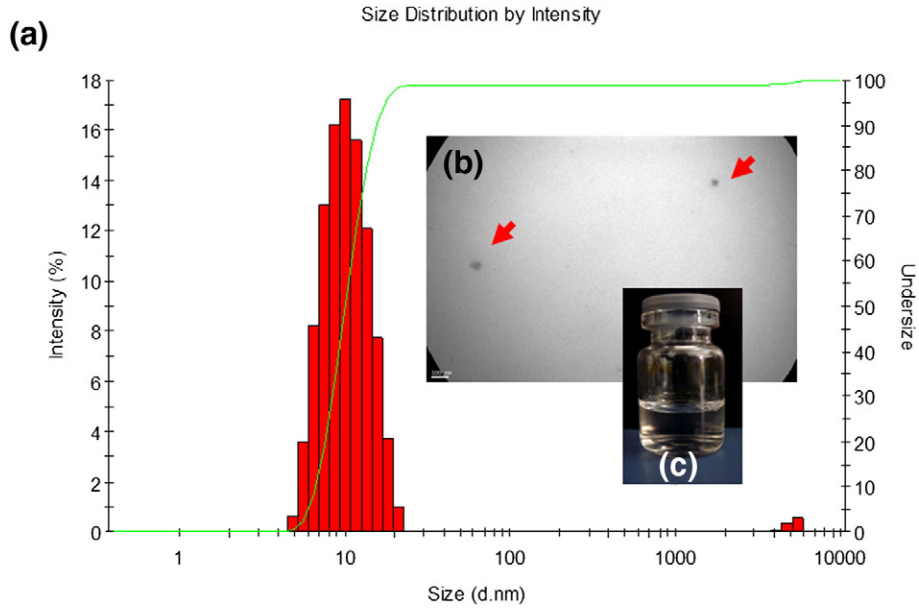

Fig. 1. Size distribution (a) and TEM micrographs (b) of TPGS nanomicelles (10% w/v), scale bar: 100 nm. (c) Macroscopic aspect of a TPGS micellar dispersion in distilled water.

Other properties explored for TPGS are: i) its ability to act as an adjuvant in vaccine systems for intranasal administration [15] and ii) its use as a nutrition supplement [16].

Recently, a new generation of multifunctional nanocarriers for simultaneous diagnosis and therapy, known as "theranostics" nanoformulations, has risen representing a new platform for personalized nanomedicines. These nanoformulations allow the assessment of drugs biodistribution and accumulation in a certain target along with the possibility of reaching therapeutic efficacy [17,18]. Labeling TPGS or any of the TPGS-based nanostructures stands as a real challenge and the first rational step toward building a true theranostic agent. This first step is evaluated in this work and further research is needed to test loading (with a therapeutic drug) and labeling of TPGS-based nanostructures altogether. In addition, small animal imaging represents a powerful tool to follow up labeled probes and could help with characterization of nanosystems as it can show *in vivo* kinetics and organ biodistribution [19,20]. These techniques can also provide information about *in vivo* stability of labeled compounds or structures. We therefore designed a method to biologically characterize TPGS-based nanomicelles by labeling them with ^{99m}Tc, a widely known and used radionuclide with diagnostic purposes in nuclear medicine [21]. Radiolabeling TPGS-based nanomicelles has an enormous potential for multiple purposes: first it can easily enlighten the pharmacokinetic and pharmacodynamic of this nanosystem by using noninvasive techniques, second it could also constitute a tumor diagnostic agent for nuclear medicine and finally and even more significant it could, potentially and with further research needed, constitute itself a theranostic agent if it is susceptible to carry a therapeutic drug and to stay labeled.

2. Materials and methods

2.1. Micelles preparation

For the TPGS nanomicelles preparation, 10 g of commercial TPGS was weighted and dissolved in 100 mL of distilled water with continuous agitation and temperature (30 °C) until a homogeneous dispersion

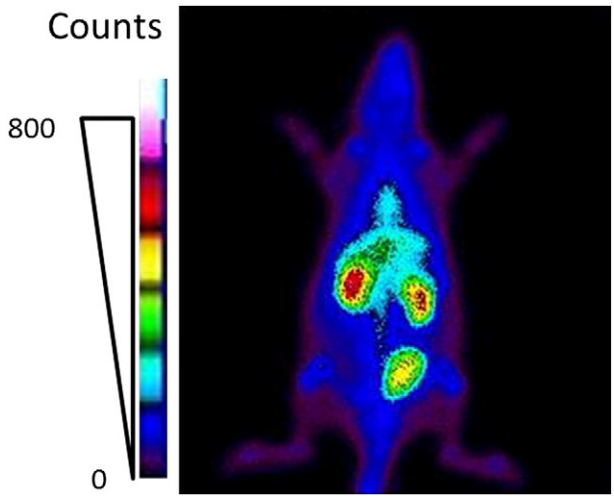

Fig. 2. Biodistribution of ^{99m}Tc radiolabelled TPGS-based nanomicelles (74 MBq). Static image was acquired 1 h post administration in ventral view (256 × 256 matrix, 1.5 zoom, ≥1.5 million counts, 20 min scan). Anesthesia: ketamine/xilazine. Color Band scale is shown.

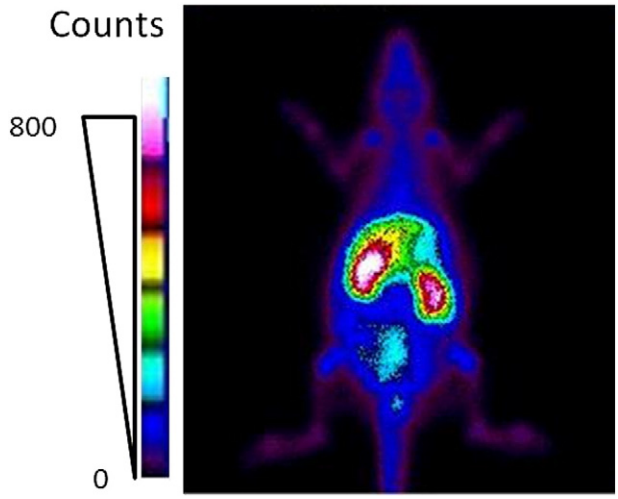

Fig. 3. Biodistribution of ^{99m}Tc radiolabelled TPGS-based nanomicelles (74 MBq). Static image was acquired 12 h post administration in ventral view (256 × 256 matrix, 1.5 zoom, ≥1.5 million counts, 35 min scan). Anesthesia: ketamine/xilazine. Color Band scale is shown.

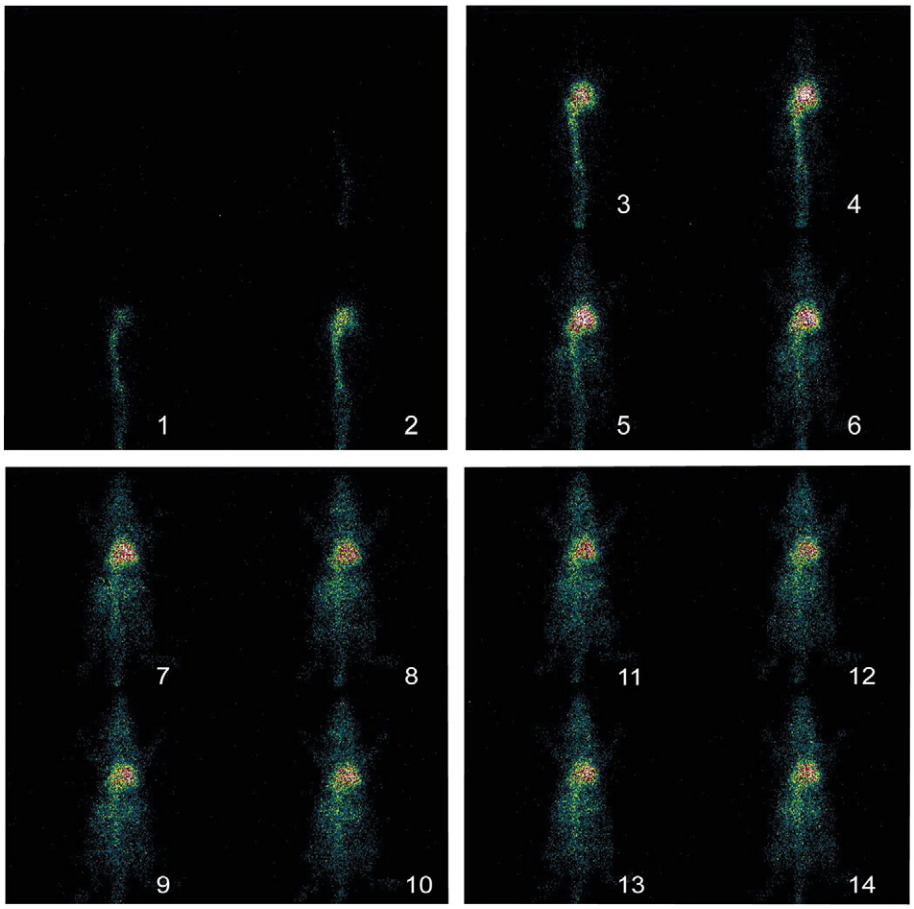

Fig. 4. Perfusion Phase of the dynamic study of ^{99m}Tc-TPGS. The study began with the radiopharmaceutical intravenous administration. Acquisitions were made as 1 s/frame (256 × 256 matrix, 1.5 zoom, 60 s). Numbers below each frame represent the seconds post injection. Anesthesia: ketamine/xilazine. Standard scale is shown.

was achieved. Then samples were equilibrated for 24 h and filtered by clarifying filters (0.2 μm, cellulose nitrate) before use. Finally, the suspension was used to perform the radiolabeling procedure.

2.2. Micellar size distribution and morphology

The average hydrodynamic diameter (D_h) of TPGS nanomicelles (10% w/v) was measured by dynamic light scattering (DLS, scattering angle of $\theta = 173°$ to the incident beam, Zetasizer Nano-Zs, Malvern Instruments, United Kingdom) at 25 °C. Samples equilibrated for 5 min at 25 °C before the measurements (n = 3 ± S.D.). The morphology of the TPGS nanomicelles (10% w/v) was characterized by transmission electron microscopy (TEM, Philips CM-12 TEM apparatus, FEI Company, The Netherlands). Briefly, aliquots were placed onto a grid and covered with Fomvar film, stained with 5 μL of phosphotungstic acid solution (1% w/v), washed with distilled water (5 μL) and dried into a silicagel container.

2.3. Radiolabeling

Labeling process was performed by a direct method as follows: a 10% w/v TPGS dispersion was incubated for 2 h with 25 mCi of $^{99m}TcO4^-$ eluted from a ^{99}Mo-^{99m}Tc generator (Laboratorios BACON, Argentina). $SnCl_2$ (Sigma-Aldrich, USA) was dissolved using HCl 6 N (Anedra, Argentina) and then added to the reaction vial reaching a concentration of 2.5 mg/mL. The radiolabeling was assessed prior to ^{99m}Tc-TPGS based nanomicelles intravenous administration by using paper chromatography: Whatman N°1 (W&R BALSTON Ltd., England) paper and methyl-ethyl-cetone (Cicarelli, Argentina) as stationary and mobile phases respectively.

2.4. Serum stability

Serum samples (3 h post injection) were assessed by paper chromatography: Whatman N°1 (W&R BALSTON Ltd., England) paper and methyl-ethyl-cetone (Cicarelli, Argentina) as stationary and mobile phases respectively.

2.5. Animals

All animal procedures were approved by the Ethical Committee for the Use and Care Laboratory Animals (CICUAL) of the School of Pharmacy and Biochemistry, Universidad de Buenos Aires (Res CD 3761/13).

Sprague Dawley rats (250–300 g) were kept in stainless steel cages under a 12 h light 12 h darkness cycle. Food and water were available *ad libitum*. Animals were anesthetized using ketamine–xilazine (90 mg/kg–5 mg/kg) [22] and placed ventrally over the collimator for the administration of 74 MBq of radioactive micelles (N = 3) or free radiolabel (N = 3) through the tail vein (intravenously). Pressure was applied until hemostasis was achieved. After dynamic imaging and 1 h static acquisition, animals were kept in the same conditions but in a specially adapted bunker until the 12 h image.

2.6. Imaging and pharmacokinetics

Small animal imaging was performed using a small field of view gamma camera (OHIONUCLEAR, Software; IM512P, ALFANUCLEAR, Argentina) equipped with a high resolution parallel hole collimator. A dynamic study was performed during the first hour post radioactive micelles administration. Then two static images were acquired in ventral position: 1 h and 12 h post injection. Dynamic study: 1 frame/s (for

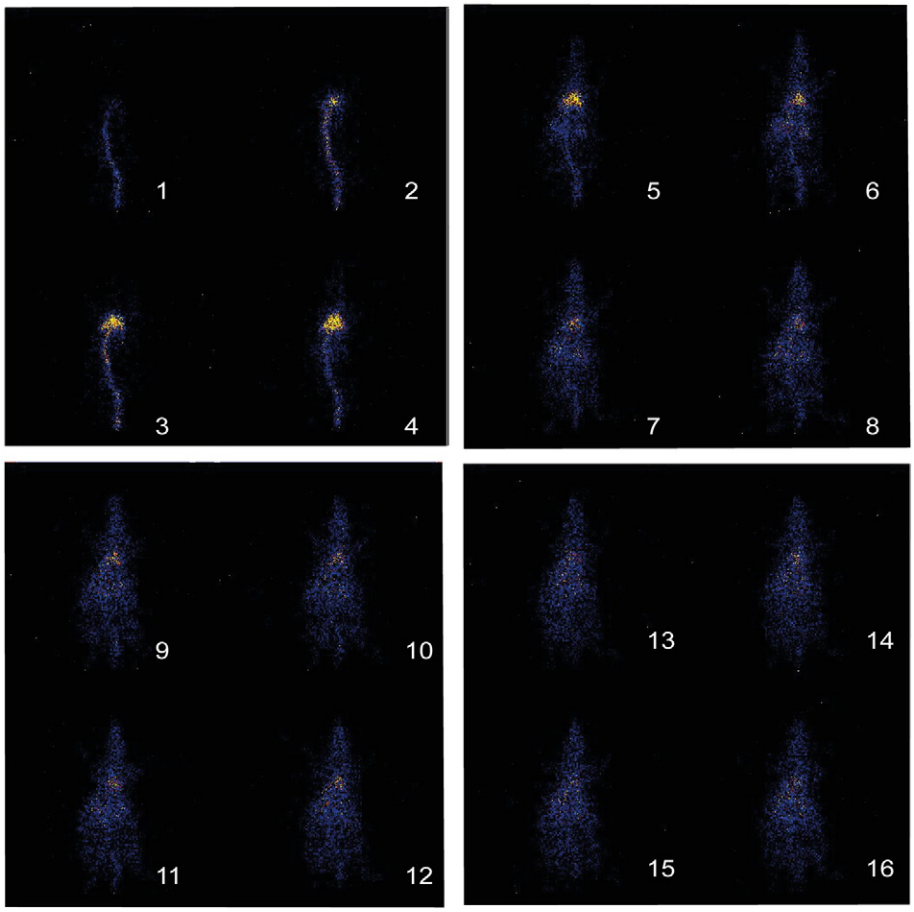

Fig. 5. Perfusion phase of the dynamic study of $^{99m}TcO_4^-$. The study began with the free label administration. Acquisitions were made as 1 frame/s (256 × 256 matrix, 1.5 zoom, 60 s). Numbers below each frame represent the seconds post injection. Anesthesia: ketamine/xilazine. Warm scale is shown.

60 s) and then 1 frame/3 min (60 min); 256 × 256 matrix, 1.5 zoom. Static studies: 256 × 256 matrix; 1.5 zoom; more than 1.5 million counts (20–35 min scan). To analyze the results regions of interest (ROIs) were created on relevant organs in order to get semi quantitative results of the radioactive micelles biodistribution and they were expressed as %Total counts (calculated as: $ROI_{counts}/Total_{counts}$x 100).

In order to correlate the imaging results with pharmacokinetics of ^{99m}Tc-TPGS based nanomicelles serum samples were taken (100 uL) at different time points post injection (10 min, 40 min, 1 h, 2 h, 3 h, 6 h, 12 h and 24 h) and radioactivity concentration was measured in a solid scintillation counter. Appropriate standards were built in order to express the results as %Injected dose.

3. Results

The spherical morphology and size of TPGS-based nanomicelles is shown in Fig. 1. The difference on micellar size between both techniques could be attributed to the micellar concentration used in this study. For the microscopy assay samples were dried, therefore, micellar aggregates could be expected since micelles are considered "dynamic systems" where their dilution can modify their hydrodynamic diameter and morphology [23,24]. Paper chromatography results revealed 95 ± 5% of the radioactivity at the strip origin, showing the success of the radiolabeling method given that the predictable impurities remain below the commonly accepted limits for this kind of probes [25]. The results of the *in vivo* stability in serum samples (98 ± 1%) were in harmony with some of the imaging results which show that radiochemical purity assay was suitable for this purpose.

Fig. 2 shows the *in vivo* localization of TPGS-based nanomicelles at 1 h post administration. Nanomicelles essentially reached heart, liver, kidneys, bone and bladder by the first hour of biodistribution. This constitutes evidence of the accumulation of the micelles in organs which have cells from reticuloendothelial system (bone marrow and liver) but it also shows a possible elimination of the renal pathway and a time dependent localization in cardiac tissue. Fig. 3 shows TPGS biodistribution after 12 h of administration, kidneys and liver increased their TPGS nanomicelles content whereas heart decreased it. A small abdominal uptake can be noticed probably due to intestinal content. Further metabolic studies should be performed in order to characterize elimination pathways and their kinetics in between the time points evaluated here and even longer ones.

Intravenous administration is a key factor when analyzing pharmacokinetics of a new nano-system. In this case, TPGS based nanomicelles were radiolabeled with ^{99m}Tc which allowed follow up of the biodistribution of the ^{99m}Tc-TPGS since its administration. Figs. 4 and 5 show the first seconds of the intravenous administration of radiolabelled nanomicelles and the free radiolabel ($^{99m}TcO_4^-$) as a control. It is noticeable the moment in which the radiopharmaceutical and the free label reach the heart (few seconds post injection) and from this moment on they began to distribute throughout the whole body. This is the perfusion phase which lasted for 1 min (only the first seconds are shown).

Figs. 6 and 7 show functional phases of ^{99m}Tc-TPGS and $^{99m}TcO4^-$ respectively. The upper panel (from 1.5 to 7 min) shows early biodistribution and the lower, the later one (from 47.5 to 53 min). There are clear and very noticeable differences among ^{99m}Tc-TPGS and the free label in their biodistribution and pharmacokinetics at the early and the latter stages. It is worth mentioning the high $^{99m}TcO4^-$

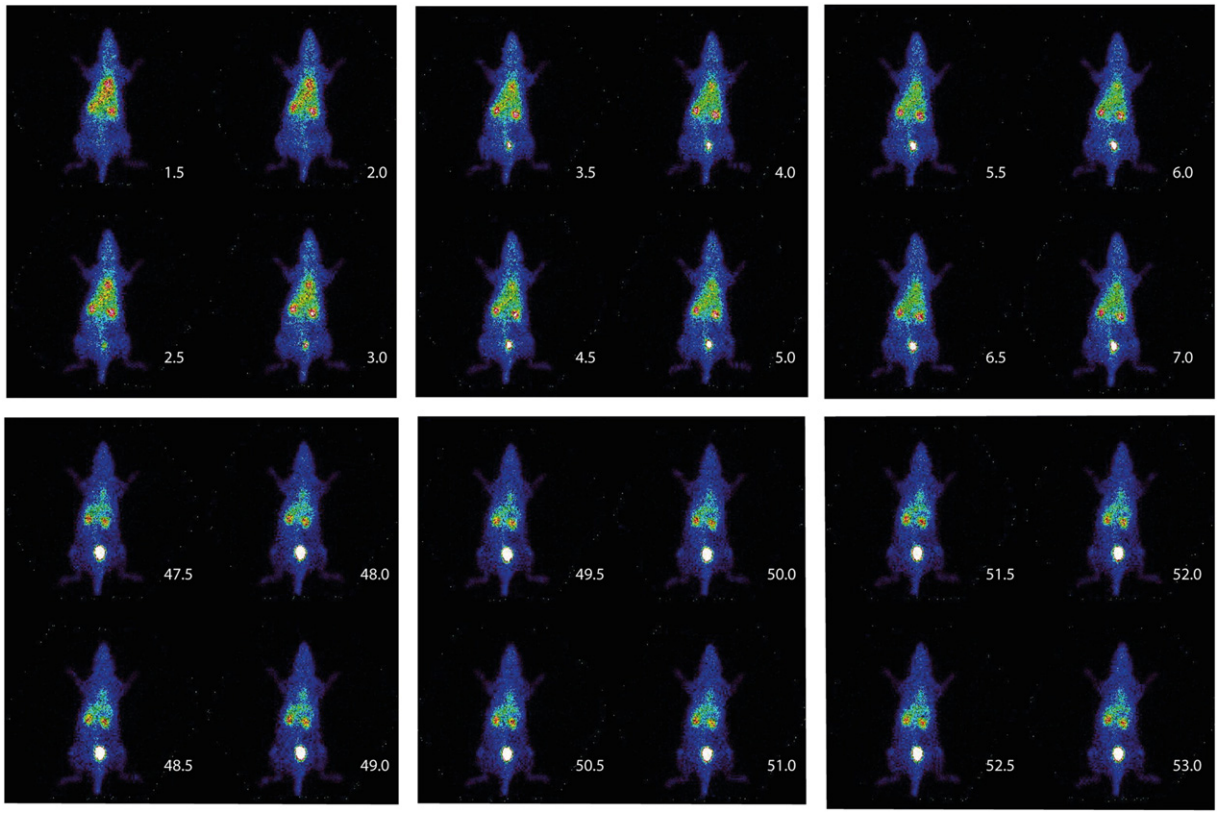

Fig. 6. Functional phase of the dynamic study of ^{99m}Tc-TPGS (37 MBq). The study began 1 min post radiopharmaceutical intravenous administration. Acquisitions were made as 30 s/frame (256 × 256 matrix, 1.5 zoom, 60 min). Numbers below each frame represent the minutes post injection. Anesthesia: ketamine/xilazine. Standard scale is shown.

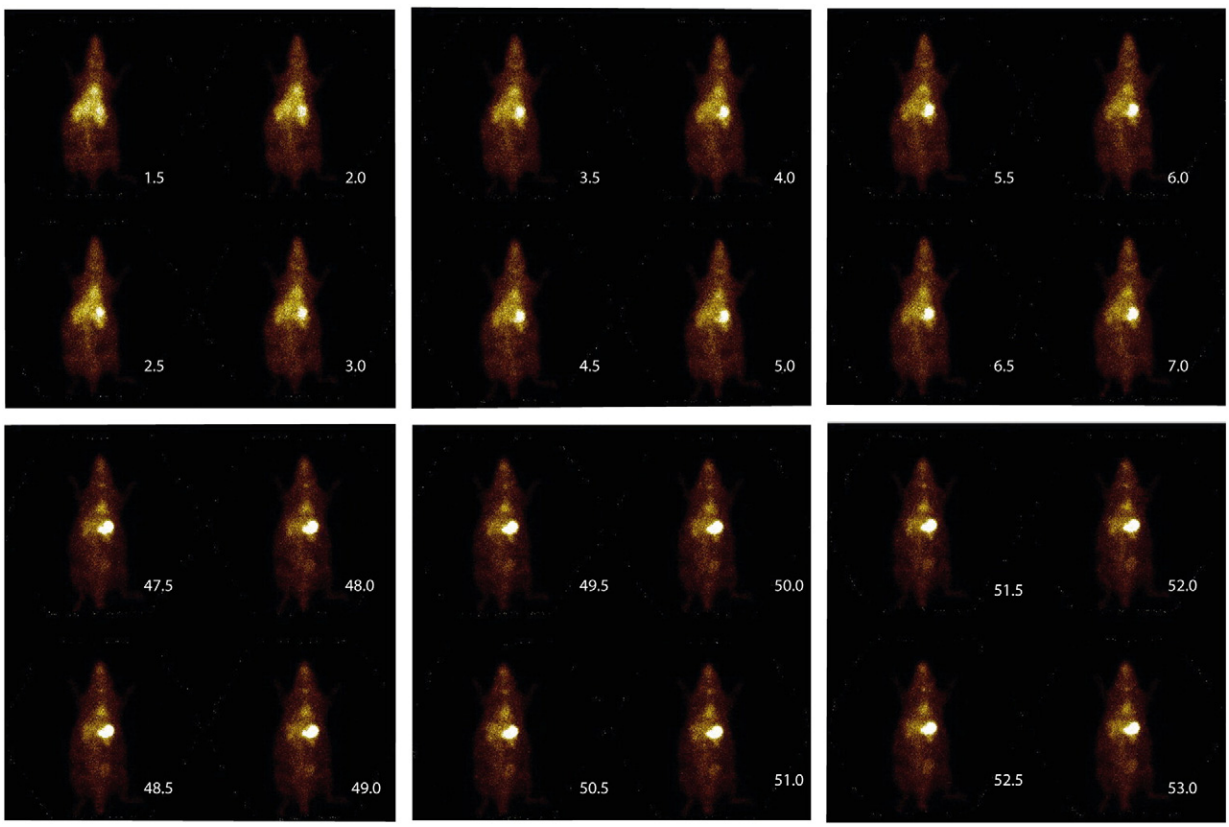

Fig. 7. Functional phase of the dynamic study of $^{99m}TcO_4^-$ (37 MBq). The study began 1 min post radiopharmaceutical intravenous administration. Acquisitions were made as 30 s/frame (256 × 256 matrix, 1.5 zoom, 60 min). Numbers below each frame represent the minutes post injection. Anesthesia: ketamine/xilazine. Yellow scale is shown.

Table 1
Semiquantification of the %Total for specific organs.

	%Total counts					
	Soft tissue	Bone	Heart	Kidneys	Liver	Background
1 h PI	6.1 ± 0.5	1.2 ± 0.2	1.5 ± 0.6	16.6 ± 1.3	8.6 ± 1.1	0.15 ± 0.01
12 h PI	3.9 ± 0.1	1.0 ± 0.1	0.7 ± 0.3	26.5 ± 1.7	11.1 ± 0.1	0.080 ± 0.002

Results were calculated by creating ROIs. Two different time points are presented: 1 and 12 h post radiolabelled nanomicelles injection (PI).

uptake in stomach and mouth. However, these two sites do not appear in ^{99m}Tc-TPGS images, proving the labeling of the nanomicelles and the absence of free radiolabel. As mentioned above, those results were predicted accurately with radiochemical purity assay. On the light of that result it can be concluded that the labeling of the TPGS nanomicelles remains stable *in vivo* (as it was also demonstrated by serum stability assay), at least until specific tissues were reached. Table 1 shows semi quantitative analysis of the organs of interest. At 12 h post injection the activity accumulated in kidneys and liver was about 40% higher than at the first hour meaning that micelles continued accumulating in both organs in a time dependent way. Bone uptake was evaluated by placing the regions of interest (ROIs) over the knees which rendered similar values at both time points. An interesting fact is that soft tissue as well as cardiac tissue had almost 50% less activity at the delayed image when compared to the early one. This could reflect that at the first hour micelles were still in circulation and 12 h later most of them were already localized in specific tissues. An extended circulating time is expected for these PEG exposing nanomicelles [26]. Moreover a two phase decay curve was fitted in ^{99m}Tc-TPGS serum concentration over time as it can be seen in Fig. 8. This means that clearance from blood has different constant rates during early time points when compared to delayed time points after administration. This shows that static images taken at 1 and 12 h were representative of both phases.

4. Discussion

It is worth mentioning the fact that placing ROIs in planar images can lead to structure superposition which is an inherent characteristic of the semiquantification performed using this technique. Some regions are more critical than others, nevertheless biological distribution results can be obtained with all the advantages of a non-invasive imaging practice.

The application of this imaging technique allows performing the biological characterization of TPGS nanomicelles, being these data useful to predict their application on different pathologies, as a potential diagnostic tool and a drug delivery system for passive or active targeting in infectious reservoirs (theranostic agent). Among the different infectious diseases which present anatomical reservoirs, extrapulmonary tuberculosis (epTB) (affecting 50% of human immunodeficiency virus (HIV)-positive patients) exhibits a skeletal/articular form (35% of epTB cases) which involves arthritis and extraspinal osteomyelitis. Also it has been described as renal tuberculosis, being the kidneys the most affected organs and tuberculous pericarditis [27,28]. In case of HIV antiretroviral therapy, the overcoming of latent HIV reservoirs throughout the body involves one of the main objectives of the present highly active antiretroviral therapy (HAART). Indeed, the gut- and rectal associated lymphoid tissue as well as the intestinal macrophages have been described as viral reservoirs for HIV type 1 [29]. Among the parasite diseases, malaria caused by *Plasmodium vivax* (a worldwide severe malaria form) also is being on the spot in the past years due to the description of infection relapse by liver hypnozoites activation. In this framework, liver accumulation of TPGS micelles could enhance the current therapy toward malaria elimination [30].

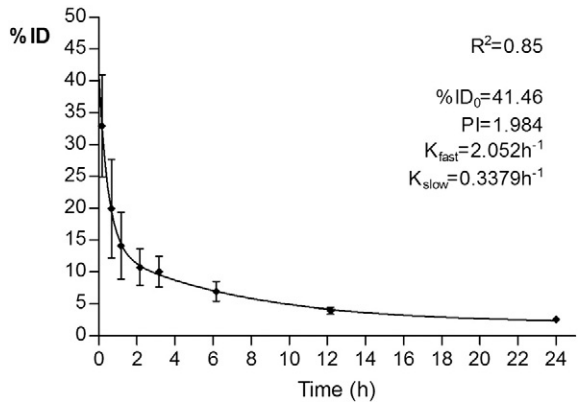

Fig. 8. Pharmacokinetics of ^{99m}Tc-TPGS based nanomicelles. ^{99m}Tc-TPGS was injected (350 μCi) intravenously by the tail vein. Serum concentration (100 μL sample) was expressed as a % Injected dose (%ID) and it is plotted as media ± SD (N = 3; error bars that cannot be seen are smaller than dots). A non-linear curve (two phase decay) was fitted and parameters are shown: constant rates for fast and slow phases (K_{fast}, K_{slow} respectively); extrapolated %Injected dose at 0 h (%ID_0); plateau: %ID value at theoretical infinite times (PI).

Thereby this radiopharmaceutical approach provides biological behavior understanding of the nanomicelles in a way no other technique does. Radionuclide based imaging contributes, in this way, to preclinical phases of new drugs or delivery systems development. The information provided and the clinical translation of this imaging technique is not comparable to any other practice. The key lays on the ability to know specific organ localization at precise time points which could help elucidate the true potentialities of this nanosystem avoiding theoretical speculations. In addition, research in this area raises awareness of the possible side effects of its administration. Serum concentration studies allow us to understand pharmacokinetics of this radiolabelled probe and to validate the imaging time points chosen. Therefore we consider them complementary studies to imaging assessment.

This work demonstrated that TPGS based nanomicelles are susceptible to be radiolabelled with ^{99m}Tc, thus they can be used to perform imaging studies in animal models. Interestingly, these novel nanosystems could be successfully employed as a potential diagnostic agent. Furthermore, commercially available FDA approved-biomaterials could offer the possibility of developed cost-viable and scalable products without the requirement of long-term/expensive biocompatibility assays. This issue stands as extremely useful for the potential bench-to-bed research translation employing TPGS as a biomaterial.

Supporting information

This work was supported by grants from the University of Buenos Aires 20020130100721BA (Director: Dr. Marcela Zubillaga, Co-Director: Dr. Jimena Salgueiro) and 20020130200038BA (Director: Dr. Diego Chiappetta).

References

[1] Crucho CIC. Stimuli-responsive polymeric nanoparticles for nanomedicine Chem. Med Chem 2015;10(1):24–38.
[2] Blanco E, Shen H, Ferrari M. Principles of nanoparticle design for overcoming biological barriers to drug delivery. Nat Biotechnol 2015;33:941–51.
[3] Bernabeu E, Chiappetta DA. Vitamin E TPGS used as emulsifier in the preparation of Nanoparticulate systems. J Biomater Tissue Eng 2013;3:122–34.
[4] Zeng X, Tao W, Mei L, Huang L, Tan C, Feng S. Cholic acid-functionalized nanoparticles of star-shaped PLGA-vitamin E TPGS copolymer for docetaxel delivery to cervical cancer. Biomaterials 2013;34:6058–67.

[5] Bernabeu E, Gonzalez L, Legaspi MJ, Moretton MA, Chiappetta DA. Paclitaxel-loaded TPGS-b-PCL nanoparticles: in VitroCytotoxicity and cellular uptake in MCF-7 and MDA-MB-231 cells versus mPEG-b-PCL nanoparticles and Abraxane®. J Nanosci Nanotechnol 2016;16:160–70.
[6] Butt AM, Iqbal MC, Amin M, Katas H. Synergistic effect of pH-responsive folate-functionalized poloxamer 407-TPGS-mixed micelles on targeted delivery of anticancer drugs. Int J Nanomedicine 2015;10:1321–34.
[7] Zhang XY, Zhang Y. Enhanced antiproliferative and apoptosis effect of paclitaxel-loaded polymeric micelles against non-small cell lung cancers. Tumor Biol 2015; 36(7):4949–59.
[8] Wang S, Chen R, Morott J, Repka MA, Wang Y, Chen M. mPEG-b-PCL/TPGS mixed micelles for delivery of resveratrol in overcoming resistant breast cancer. Expert Opin Drug Deliv 2015;12(3):361–73.
[9] Dou J, Zhang H, Liu X, Zhang M, Zhai G. Preparation and evaluation in vitro and in vivo of docetaxel loaded mixed micelles for oral administration. Colloids Surf B Biointerfaces 2014;114:20–7.
[10] Mu L, Elbayoumi TA, Torchilin VP. Mixed micelles made of poly(ethylene glycol)-phosphatidylethanolamine conjugate and D-α-tocopheryl polyethylene glycol 1000 succinate as pharmaceutical Nanocarriersfor Camptothecin. Int J Pharm 2005;306:142–9.
[11] Li P, Lai P, Hung W, Syu W. Poly(l-lactide)-vitamin E TPGS nanoparticles enhanced the cytotoxicity of doxorubicin in drug-resistant MCF-7 breast cancer cells. Biomacromolecules 2010;11(10):2576–82.
[12] Shi C, Zhang Z, Wang F, Ji X, Zhao Z, Luan Y. Docetaxel-loaded PEO– PPO–PCL/TPGS mixed micelles for overcoming multidrug resistance and enhancing antitumor efficacy. J Mater Chem B 2015;3:4259–71.
[13] Huang S, Yu X, Yang L, Song F, Chen G, Lv Z, et al. The efficacy of nimodipine drug delivery using mPEG-PLA micelles and mPEG-PLA/TPGS mixed micelles. Eur J Pharm Sci 2014;63:187–98.
[14] Moretton MA, Taira C, Flor S, Bernabeu E, Lucangioli S, Höcht C, et al. Novel nelfinavir mesylate loaded d-α-tocopheryl polyethylene glycol 1000 succinate micelles for enhanced pediatric anti HIV therapy: in vitro characterization and in vivo evaluation. Colloids Surf B Biointerfaces 2014;123:302–10.
[15] Somavarapu S, Pandit S, Gradassi G, Bandera M, Ravichandran E, Alpar OH. Effect of vitamin E TPGS on immune response to nasally delivered diphtheria toxoid loaded poly(caprolactone) microparticles. Int J Pharm 2005;298:344.
[16] Jacquemin E, Hermeziu B, Kibleur Y, Friteau I, Mathieu D, Le Coz F, et al. Bioavailability of oral vitamin E formulations in adult volunteers and children with chronic cholestasis or cystic fibrosis. J Clin Pharm Ther 2009;34:515–22.
[17] Janib SM, Moses AS, MacKay JA. Imaging and drug delivery using theranostic nanoparticles. Adv Drug Deliv Rev 2010;62:1052–63.
[18] Kumar R, Kulkarni A, Nagesha DK, Sridhar S. In vitro evaluation of theranostic polymeric micelles for imaging and drug delivery in cancer. Theranostics 2012;2:714–22.
[19] Willmann JK, van Bruggen N, Dinkelborg LM, Gambhir SS. Molecular imaging in drug development. Nat Rev Drug Discov 2008;7:591–607.
[20] Peremans K, Cornelissen B, Van Den Bossche B, Audenaert K, Van de Wiele CA. Review of small animal imaging planar and pinhole spect gamma camera imaging. Vet Radiol Ultrasound 2005;46:162–70.
[21] Saha GB. Fundamentals of nuclear pharmacy. 5th ed. New York: Springer-Verlag; 2004.
[22] Hein M, Roehl AB, Tolba RH. Animal anesthesia and monitoring. In: Kiessling F, Pichler BJ, editors. Small animal imaging. Berlin: Springer-Verlag; 2011. p. p83–92.
[23] Owen SC, Chan DPY, Shoichet MS. Polymeric micelle stability. Nano Today 2012;7:53–65.
[24] Allen C, Maysinger D, Eisenberg A. Nano-engineering block copolymer aggregates for drug delivery. Colloids Surf B Biointerfaces 1999;16:3–27.
[25] Bringhammar T, Zolle I. Quality Assurance of Radiopharmaceuticals. In: Zolle I, editor. Technetium-99 m pharmaceuticals. Preparation and quality control in nuclear medicine. Berlin Heidelberg: Springer; 2007. p. 67–71.
[26] Moghimi SM, Hunter AC, Murray JC. Long-circulating and target-specific nanoparticles: theory to practice. Pharmacol Rev 2001;53(2):283–318.
[27] Fanlo P, Tiberio G. Extrapulmonary tuberculosis. An Sist Sanit Navar 2007;30:143–62.
[28] Golden MP, Vikram HR. Extrapulmonary tuberculosis: an overview. Am Fam Physician 2005;72:1761–8.
[29] Cory TJ, Schacker TW, Stevenson M, Fletcher CV. Overcoming pharmacologic sanctuaries. Curr Opin HIV AIDS 2013;8:190–5.
[30] Wells TNC, Burrows JN, Baird JK. Targeting the hypnozoite reservoir of plasmodium vivax: the hidden obstacle to malaria elimination. Trends Parasitol 2010;26:145–51.